Mon. Not. R. Astron. Soc. **000**, 000–000 (0000) Printed 8 October 2013 (MN LATEX style file v2.2)

# The place of the local group in the cosmic web

Sebastian Bustamante ⋆[1] Jaime E. Forero-Romero[2]

[1] *Instituto de Física - FCEN, Universidad de Antioquia, Calle 67 No. 53-108, Medellín, Colombia*
[2] *Departamento de Física, Universidad de los Andes, Cra. 1 No. 18A-10, Edificio Ip, Bogotá, Colombia*

8 October 2013

**ABSTRACT**

We present here a study about the influence of the environment on the local group (LG) of galaxies in the context of ΛCDM. In this study we use a large volume high resolution N-body cosmological simulation (Bolshoi) together with the most recent methods to quantify the cosmic web (T-web, V-web schemes); furthermore we propose a novel approximation, base upon the minimization of the mean density of void regions, to determinate the optimum threshold value $\lambda_{th}$, which have been treated until now as a free parameter. Following the recent work of Courtois et al. (2013), where was found that the LG is located near to a large void, we also do an extensive study of voids, applying a FOF algorithm to find void regions and performing an analysis of their shape based upon the reduced inertia tensor. Using the recent observations that constrained the tangential velocity of M31 with respect to the Milky Way (MW), the previously established radial velocity, the estimated masses of dark halos, along with some criteria to guarantee the gravitational isolation of these systems (Forero-Romero et al. 2013-1), we select a set of halos pairs as a representative sample of LG systems in the Bolshoi simulation. We look for possible bias and correlations between the environment properties of each LG system and its kinematic and formation properties. Among our main result we find **[summarize our results here!]**.

**Key words:** Cosmology: large-scale Structure of Universe, galaxies: star formation - line: formation

## 1 INTRODUCTION

The spatial distribution of galaxies describes a web-like pattern, the so-called cosmic web. Today it is understood that such configuration is driven by gravitational instabilities. ...

The study of the influence of the cosmic web on galaxy properties start with the seminal work of Dressler **[reference here]** and extends to recent works using large observational surveys that look for signatures of the web into the evolution of galaxy populations. With the advention of more detailed observations and sophisticated computational models it is now within our reach to understand what physical processes dominate.

This makes that the mass assembly history of a galaxy is deeply connected with its position in the cosmic web. There is an extensive body of literature on the effects of the web environment on the observable properties of galaxies.

This environmental study is also of paramount importance to understand the formation of our Galaxy. In our local neighborhood, the observations of dwarf galaxies around the Milky Way (MW) and the Andromeda galaxy (M31) show filamentary and disk-like patterns that can be linked to a preferential infall direction, very likely connected with the cosmic web where the Local Group (LG) of galaxies is embedded.

In this paper we quantify the velocity shear environment of DM halo pairs representative of the principal members of the Local Group (LG), the Milky Way (MW) and Andromeda galaxy (M31). We perform this study in an unconstrained cosmological simulation from random phases in the initial conditions, and unlike previous works, where were used constrained cosmological simulations which have been setup as to reproduce the large scale structure of the local universe, we use directly observational measurements of the kinematics properties of the local group **[Reference here]** in order to build faithful samples of LG-like systems.

We pay special attention to the correlation of the present velocity shear environment with the assembly and the kinematics properties of the pairs. The motivation to have that focus is that it has been previously shown that the LG present in three different realizations of the constrained simulations have assembly histories biased towards

⋆ sbustama@pegasus.udea.edu.co

early formation times and absence of major mergers (ratio 1:10) in the last 10 Gyr. In the case of the kinematic properties, recent observational constrains to the galactocentric tangential velocity of M31 has enabled to establish how typical is the LG in a cosmological context [reference to Forero-Romero et.al 2013-1], that is why we focus here how a specific kind of host environment biases these kinematics properties.

## 2 THE SIMULATION

As it was previously mentioned, we use an unconstrained cosmological simulation, the Bolshoi simulation, to identify the possible large scale environment of the Local Group. This is a similar approach to the one already used by [reference here].

The Bolshoi simulations follows the non-linear evolution of a dark matter density field on a cubic volume of size $250h^{-1}$Mpc sampled with $2048^3$ particles. The cosmological parameters in the simulation are $\Omega_{\rm m} = 0.27$, $\Omega_\Lambda = 0.73$, $h = 0.70$, $n = 0.95$ and $\sigma_8 = 0.82$ for the matter density, cosmological constant, dimensionless Hubble parameter, spectral index of primordial density perturbations and normalization for the power spectrum. The mass of each particle in the simulation is $m_{\rm p} = 1.4 \times 10^8 h^{-1}{\rm M}_\odot$.

### 2.1 Halos and Merger Trees

We identify halos with two algorithms, the Friends-of-Friends [reference here] algorithm and the Bound Density Maximum algorithm. The constructed catalogues also provide the basis for the mass aggregation history studies. We also include in the catalogues information about the substructure.

All the results presented here must be interpreted in term of host halos, without any information of the substructure. In particular the merger of two FOF halos corresponds to the epoch of first overlap, and not to the fusion and/or disruption of an accreted sub-halo with a dominant halo.

The linking length is $b = 0.17$ times the mean inter-particle separation. All objects with 20 particles or more are considered a bona fide halo and are included in the construction of the merger tree, this corresponds to a minimum halo mass of $M_{\rm min} = 2.70 \times 10^9 h^{-1}{\rm M}_\odot$in the Bolshoi simulation.

The halo identification for the simulation was done for XX snapshots in the redshift range $0 < z < 7$ more or less evenly spaced in look-back time.

## 3 ALGORITHMS TO QUANTIFY THE COSMIC WEB

### 3.1 The tidal web (T-web)

The first algorithm we use to identify the cosmic web is based upon the diagonalization of the tidal tensor, defined as the Hessian of a normalized gravitational potential

$$T_{\alpha\beta} = \frac{\partial^2 \phi}{\partial x_\alpha \partial x_\beta} \tag{1}$$

where the physical gravitational potential has been rescaled by a factor $4\pi G\bar{\rho}$ in such a way that $\phi$ satisfies the following equation

$$\nabla^2 \phi = \delta, \tag{2}$$

where $\bar{\rho}$ is the average density in the Universe, $G$ is the gravitational constant and $\delta$ is the dimensionless matter overdensity.

### 3.2 The velocity web (V-web)

We also use a kinematical method to define the cosmic-web environment in the simulation. The method has been thoroughly described in XXX and applied to study the shape and spin alignment in the Bolshoi simulation here XX. We refer the reader to these papers to find a detailed description of the algorithm, its limitations and capabilities. Here we summarize the most relevant points for the discussion.

The V-web method for environment finding is based on the local shear tensor calculated from the smoothed DM velocity field in the simulation. The central quantity is the following dimensionless quantity

$$\Sigma_{\alpha\beta} = -\frac{1}{2H_0}\left(\frac{\partial v_\alpha}{\partial x_\beta} + \frac{\partial v_\beta}{\partial x_\alpha}\right) \tag{3}$$

where $v_\alpha$ and $x_\alpha$ represent the $\alpha$ component of the comoving velocity and position, respectively. $\Sigma_{\alpha\beta}$ can be represented by a $3 \times 3$ symmetric matrix with real values, that ensures that is possible to diagonalize and obtain three real eigenvalues $\lambda_1 > \lambda_2 > \lambda_3$ whose sum (the trace of $\Sigma_{\alpha\beta}$) is proportional to the divergence of the local velocity field smoothed on the physical scale $\mathcal{R}$.

The relative strength of the three eigenvalues with respect to a threshold value $\lambda_{th}$ allows for the local classification of the matter distribution into four web types: voids, sheets, filaments and peaks, which correspond to regions with 3, 2, 1 or 0 eigenvalues with values larger than $\lambda_{th}$. Below we shall discuss a novel approach to define an adequate threshold value based on the visual impression of void regions, furthermore we study other possible values based on other visual features of the cosmic web.

### 3.3 The cosmic web in Bolshoi

Both established schemes to quantify the cosmic web depend on continuous and smooth physical quantities, as the peculiar velocity field and the density field. In order to calculate the necessary tensors, a discretization of the simulation volume is performed, so all the properties are reduced to single values associated to discrete cells. According to this, we divide the overall volume into $(256)^3$ cells, so each cell has an associated comovil cubic volume of 0.98 Mpc $\rm h^{-1}$. Finally, to reduce possible effects due to the discretization process, a gaussian softening is performed between neighbour cells.

Once defined the numerical details about the classification schemes, we shall analyse the dependence on the threshold value $\lambda_{th}$ for each one. In the figure 1 we show the variation of the mean density parameter $\delta$ with the threshold value for cells marked in each of the adopted types of environment.

As was previously established by **Hoffman et al. (2012)** and as can be seen in the figure 1, the behaviour of the V-web scheme is significantly more sensible to variations of the $\lambda_{th}$ value compared with the T-web scheme; nevertheless, the behaviour of the mean density parameter for voids, sheets and filaments, are qualitatively quite similar for the two schemes, reaching extreme values in the marked $\lambda_{th}$ critical values respectively. For instance, voids reach a minim value at some critical threshold, increasing for higher threshold values, while sheets and filaments reach a maxim value at other critical threshold, decreasing for higher threshold values. Although we shall focus our analysis on voids because they are completely dominant in the visual impression of the cosmic web, an analogous analysis might be performed for other type of environments.

On cosmic scales, the presence of highly non-linear structures implies the existence of very vast regions with density lower than the mean cosmological value due to the mass conservation. That is why the visual impression of the cosmic web must be necessarily dominated by these underdense regions. Keeping that in mind, our novel proposal is based upon the correct quantification of these regions, so the optimum threshold value must be chosen such that: sheet regions do not invade real void regions (in such case, the mean density parameter of sheet regions would become negative) and void regions do not invade real sheet and filament regions (in such case, the mean density parameter of void regions would increase due to the contribution of over-dense regions). Thus, the optimum value is simply where the mean density parameter of void regions is minimized. According to this, we obtain the next threshold values for the T-web and the V-web respectively, $\lambda_{th}^{T} = 0.61$ and $\lambda_{th}^{V} = 0.26$. To verify our analysis, we show in the figure 2 the visual impression for each defined critical value, and as can be seen, the chosen values reproduce properly the expected impression according to the density field.

Our classification scheme may be thought as a refinement of the recent schemes, where the threshold value is used to taking as a free parameter, based on the classic methods, where the classification is performed based on a cut off of the density field directly **[references here]**. So we make use of the objectivity achieved by the analysis of the mean density, but keeping all the environmental information provided by the tensorial schemes instead of the poor description provided by the density field.

### 3.4 Method to find void regions

Following the recent work of **Courtois et al. 2013**, we use a method based on a FOF algorithm to find extended regions of voids in order to select halo systems according to the proximity to those regions. To achieve this, we build the input catalogue of the FOF method with the positions of the center coordinate of every cell marked as void according to the web scheme adopted; furthermore we set an adequate linking length to connect even diagonal neighbour cells.

Following the work of **Forero-Romero et al. 2008**, we also perform a percolation analysis in order to select the best threshold parameter that reduce percolation in cells, thereby accounting for physical void regions. In the figure 3 we show the obtained result of our percolation analysis for both web schemes. In both cases it can be noted the volume of the largest void region is minimized and the volume distribution of voids is relatively flat at $\lambda_{th} = 0.0$, that means percolation is completely reduced for this threshold value. So despite of the previously established $\lambda_{th}$ optimum values for each scheme, we shall use $\lambda_{th} = 0.0$ just for the detection of void regions. Besides, due to the domination of the large scale visual impression by voids, it is inevitable the presence of percolation phenomenon, so the current chosen threshold value for percolation is justified because in spite of voids are necessarily connected, we are just interested in detecting bulk regions.

Next, we shall calculate the reduced inertia tensor of each void region in order to determinate their principal directions of inertia and analyse the size-shape distribution of voids.

$$\tau_{ij} = \sum_{l} \frac{x_{l,i} x_{l,j}}{R_l^2} \tag{4}$$

where $l$ is a index associated to each cell of to the current region, $i$ and $j$ indexes run over each spatial direction and finally $R_l$ is defined as $R_l^2 = x_{l,1}^2 + x_{l,2}^2 + x_{l,3}^2$, all positions are measured from the respective center of mass of the region.

The eigenvalues of the reduced inertia tensor, i.e. the principal moments of inertia, are used to quantify the shape of void regions. They are denoted as $\tau_1$, $\tau_2$ and $\tau_3$ such that $\tau_1 \leq \tau_2 \leq \tau_3$. In the figure 4 we show the computed distributions for $\tau_1/\tau_2$ and $\tau_2/\tau_3$, where we rather calculate histograms for these ratio quantities instead of each value in order to avoid using an arbitrary normalization. For both schemes, it can be noticed that the shape-distribution is completely spread out, thereby indicating a non-preferred geometry of void regions, which is in agreement with the well-established anisotropic flow of matter associated to this type of region **[reference here]**. Because of that, we shall look for possible alignments between the plane of rotation of halo pairs and the principal directions of inertia of the nearest void regions.

## 4 LOCAL GROUP SAMPLE DEFINITION

In order to establish an adequate set of criteria to define LG samples in unconstrained simulations, we proceed from the the general dark halo catalogues, constructed using the FOF scheme with a linking length of $b = 0.17$. These samples are defined for all simulation and will be referred as General Halos (GH) samples. To be consistent with the observationally determined mass range of halos that host disk-form galaxies, we select the halos in the mass range $5 \times 10^{11} < M_h/h^{-1}\mathrm{M}_{\odot} < 5 \times 10^{12}$, referred here as Individual Halos (IH) samples.

As a primal approach to define gravitational bounded halo pairs we select all halo pairs in IH samples that satisfied to be the closest to each other, they constitute the Pairs (P) samples. To keep the concordance with previous works in algorithms for LG selection (**[references here]**), we define here the next list of conditions that have to fulfill a pair system in order to construct the Isolated Pairs (IP) samples. All these considerations are based upon the relative dynamics of the Milky Way and M31, and its isolation from massive structures:

(i) The distance between the center of the two halos should be less than $0.7h^{-1}$Mpc .

(ii) The relative physical velocity between the two halos has to be negative.

(iii) The distance to any halo more massive than any of the pair members must be less than $2h^{-1}$Mpc .

(iv) The distance to cluster-like halos with masses larger than $1 \times 10^{13}$ $h^{-1}\mathrm{M}_{\odot}$must be larger than $5h^{-1}$Mpc .

In the case of a constrained simulation one can define samples of LG systems based upon the next condition

(v) The Local Group pair must be located in the right environment with respect to the XX Cluster.

Due to the intrinsic nature of constrained simulations, we expect that these LG samples be the most faithful systems that resemble the properties and the environment of our LG. In fact, the three CLUES simulations appear to present a common T-web/V-web environment for LG systems, such as shown in the figure **??**. Based in this we propose a new criteria of selection to define more realistic LG systems in the unconstrained simulation, this consists in tanking the extreme values of each V-web/T-web eigenvalue associated to the host environment of the three LG systems in CLUES. With this range established (see table 1) we filter the IP sample in Bolshoi simulation in order to build the samples Constructed Local Groups V-web based (CLGV) and T-web based (CLGT). Finally in the table **??** we show the sizes of all defined samples for each simulation.

## 5 FINDING A LOCAL GROUP ENVIRONMENT

In this section we prepare some numerical experiments with the halos samples and their environment, with special emphasis on the isolated pairs and LG samples. All this in order to find for environment correlations and common properties between LG systems.

### 5.1 Comparison of the two simulations

Prior to study of isolated and LG samples and to determinate possible correlations between their properties, it is necessary to establish the equivalence between all simulations that we will use, with the aim to eliminate effects due to construction process of each one.

In first place, we analyse the mass distribution of individual halos and in next figure we show the integrated mass function (IMF) for halos sample with $M \geq 1 \times 10^{11} M_{\odot}$.

Although in high masses the IMF of each simulation are slightly different, in low mass region, where the most halos of our interest are, the IMFs are quite similar indicating that the sample of halos in each simulation have the same mass distribution, while the small differences are due to finite size of samples. Another aspect in the figure **??** is the position of LG halos, they are distributed across the mass range of halos that we have set (see in section 4), indicating that there is not an apparent condition with their individual masses.

The situation is quite different respect to mass ratio index of isolated pairs sample (MRI). In the figure **??** (a) we show the integrated distribution of MRI, where the approximately linear behaviour indicates an uniformly distribution. The interesting aspect here is the closeness between the LG sample values, indicating a possible common property in these systems, even though this could be established a priori by construction. In the **??** (b) is plotted the integrated distribution of total pair mass, and again like the IMF, there is not a preferential value.

Once established the concordance between the defined samples, we proceed to analyse the distribution of the eigenvalue of shear velocity tensor 3, for this we assume that the halos are good tracers of the environment properties and therefore we evaluate each eigenvalue in the center mass of each halo, mapping of this way the complete distribution (figure **??**). The black curves correspond to the unconstrained simulation (Bolshoi) and the color curves to the constrained simulations (CLUES), aditionally we calculate the cosmic variance, showed in purple curves, dividing the Bolshoi volume in smaller parts with a size comparable to the CLUES volume ($64h^{-1}$ Mpc of side). What is interesting here is the clear difference between the eigenvalues distributions of the both types of simulations, inclusively the constrained distributions does not match between the cosmic variance, indicating that although both simulations were made with the same cosmology (see subsections **??** and **??**), the constrained simulations have a significantly different environment properties (spatial matter distribution) compared to the average expected from a random volume with the same comoving size.

### 5.2 Defining the LG environment

With the aim of constructing a sample of LG systems in Bolshoi simulations, we use the eigenvalues of the three LG systems in each CLUES simulation and choose a range for each one based in the extreme values of the six halos, this with the expectation of reproducing the LG specific conditions in constrained simulations. This criteria can be thought as a first approximation to establish a more faithful sub-sample into the isolated pairs. In table 1 we show the used extreme values for each eigenvalue of local shear tensor.

As a self-consistency test, we apply this criteria to CLUES simulations and find, on average, three LG systems in each one. But to avoid confusion, we keep defining the LG sample as the three initial pairs. Finally, we construct the LG sample of Bolshoi, where the sample size is illustrated in Table **??**.

Once we have established the equivalence of samples in each simulation and have defined the LG samples, we proceed to calculate correlations between halo samples and their environment. As was mentioned in section 3.2, we do not use an specific value of eigenvalue threshold $\lambda_{th}$, instead of this, we explore a relatively wide range of this parameter (i.e. $0 \leq \lambda_{th} \leq 1$) and calculate distributions respect to each eigenvalue individually.

At first place, we calculate the environment of each LG system in CLUES simulations, for this we use the $\lambda_{th}$ scheme to classify it in void, sheet, filament or knot (see 3.2), with $\lambda_{th}$ into the threshold range. Figure **??** is obtained.

At first place, we calculate the integrated distribution of each eigenvalue for individual halos, isolated pairs and LG samples. For this, we associate to each halo a value of

environment (set of eigenvalues) according to its center of mass position in a smoothed grid ($256^3$ cells for Bolshoi and $64^3$ for CLUES, or equivalently a resolution of 1.0Mpc $h^{-1}$ per cell, according to the physical size of the pairs.)

## 6 RESULTS

### 6.1 Bias induced on kinematic and dynamics properties

... Total Mass
- ... Radial vs. tangential velocities
- ... Angular Momentum
- ... Total Mechanical energy.
- ... Reduced Spin

### 6.2 Bias induced on the Mass Assembly Histories

... Last major merger. Formation Time. Assembly Time.

### 6.3 Pair Alignment with the Cosmic Web

... Separation.
- ... Relative velocity.
- ... Angular Momentum.

## 7 CONCLUSIONS

**ACKNOWLEDGMENTS**

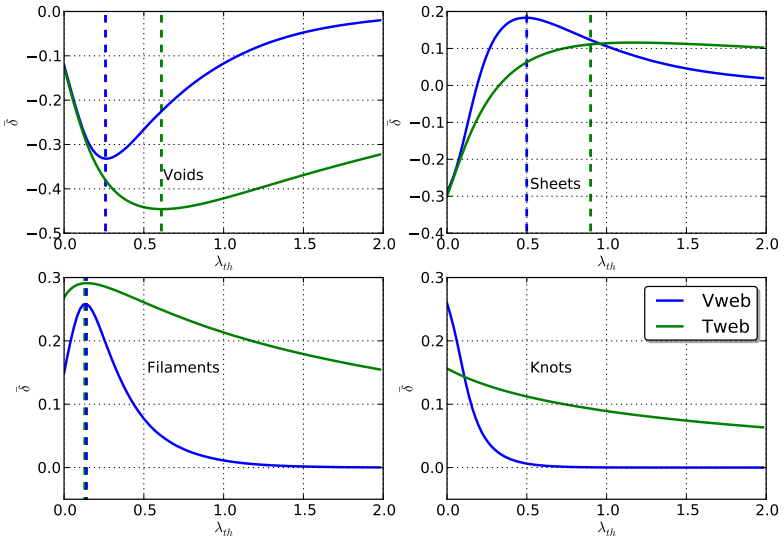


**Figure 1.** Mean density parameter for each of the defined environments according to the chosen $\lambda_{th}$ value and for both classification schemes.

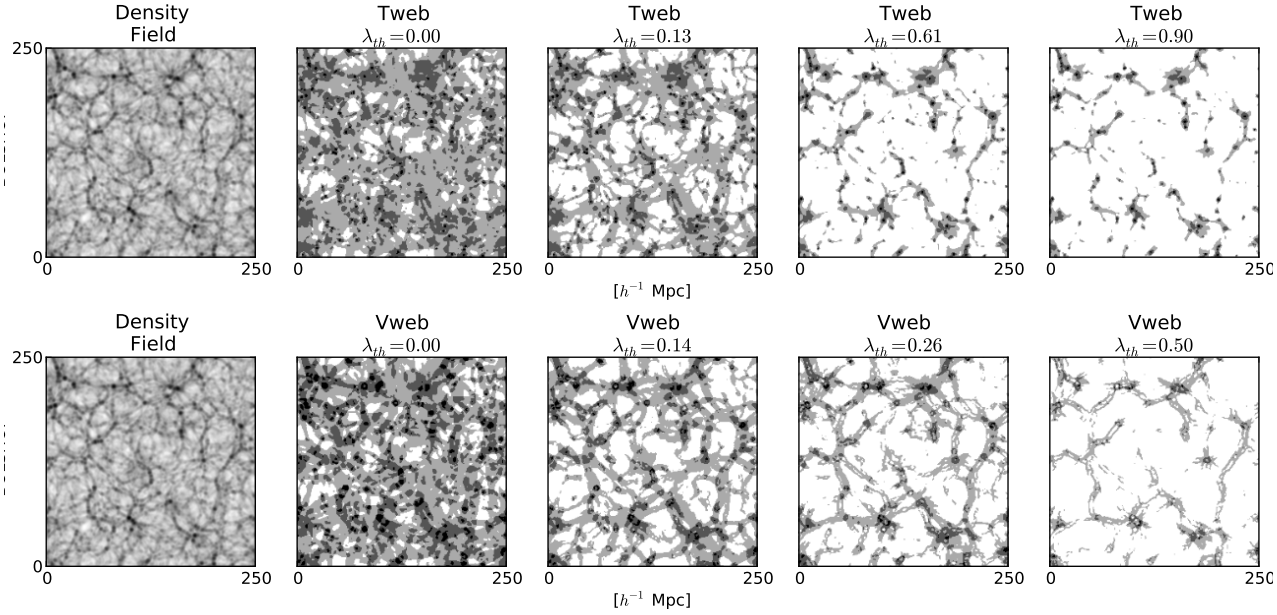


**Figure 2.** Visual impression of the density field (left), and of each classification scheme with the $\lambda_{th}$ values obtained by our criteria (others). Our color convention for each environment is (white) - void, (light gray) - sheet, (gray) - filament, (black) - knot.

| | $\boldsymbol{\lambda_1}$ $[10^{-1}]$ | $\boldsymbol{\lambda_2}$ $[10^{-1}]$ | $\boldsymbol{\lambda_3}$ $[10^{-1}]$ |
|---|---|---|---|
| **Minim value** | 1.78 | $-6.29\times10^{-2}$ | -1.98 |
| **Maxim value** | 3.49 | 1.21 | $-8.85\times10^{-1}$ |

**Table 1.** Extreme values for each V-web eigenvalues to construct LG samples.

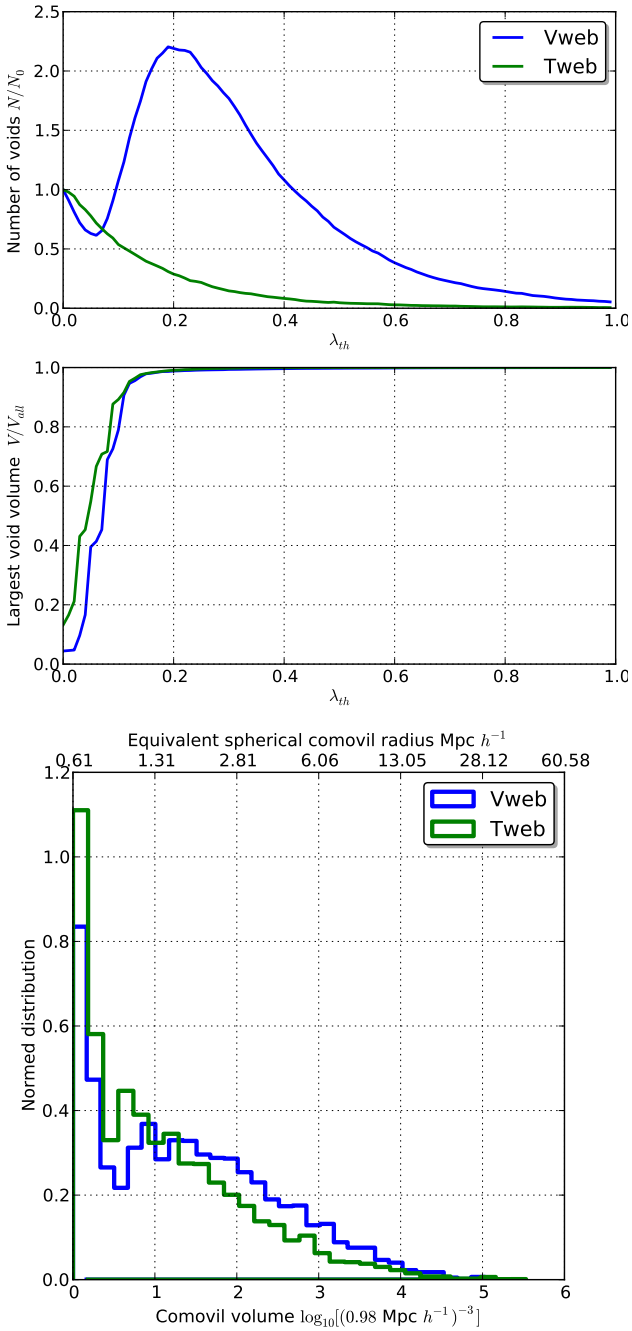


**Figure 3.** Percolation analysis of void regions for different $\lambda_{th}$ values and for both defined classification schemes.

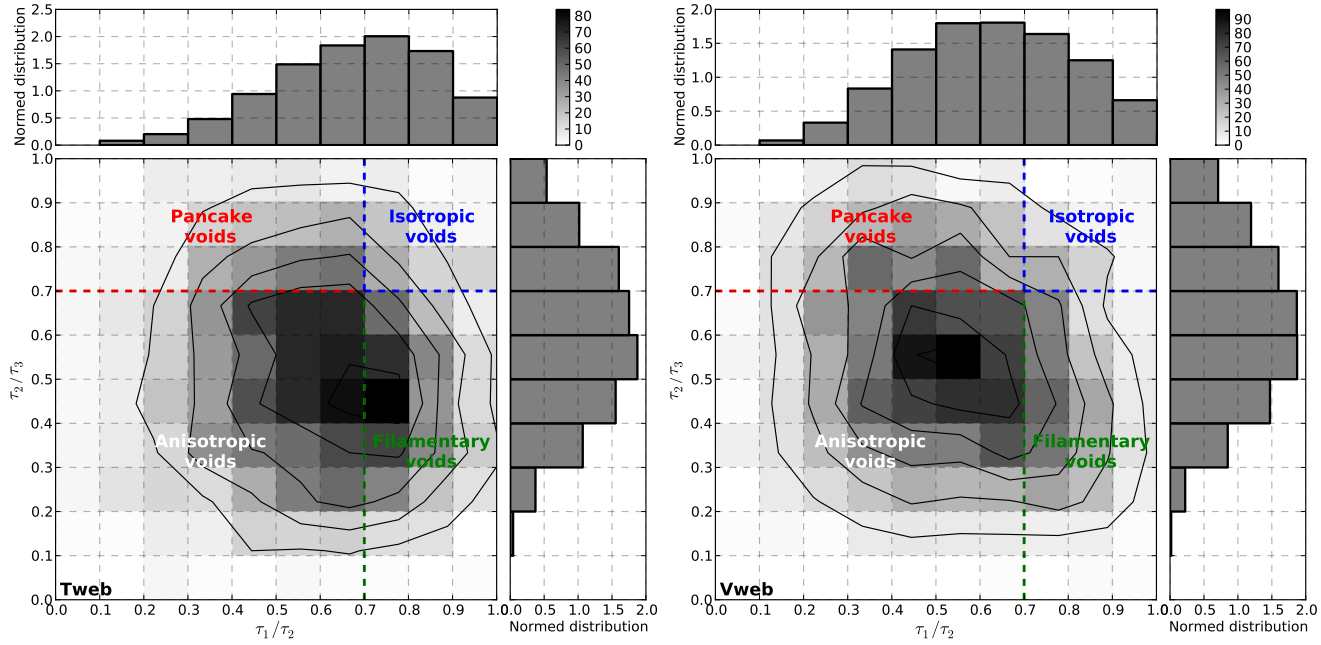


**Figure 4.** Histogram of eigenvalue ratio $\tau_1/\tau_2$ vs $\tau_2/\tau_3$ for the inertia tensor of void regions. T-web scheme (left). V-web scheme (right).

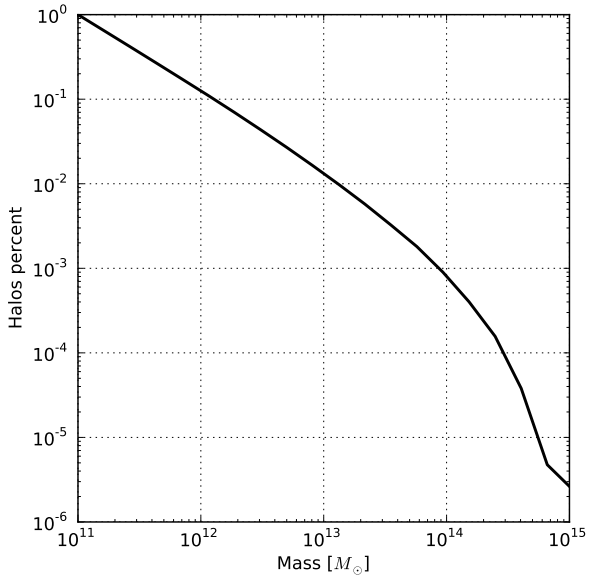


**Figure 5.** Integrated mass function of individual halos of Bolshoi.